2006

Growth and thermal properties of Sr W O 4 single crystal

J. D. Fan

H. J. Wang

M. H. Jiang

Robert I. Boughton
Bowling Green State University, boughton@bgsu.edu

D. G. Ran

See next page for additional authors

Growth and thermal properties of Sr W O 4 single crystal

J. D. Fan, H. J. Zhang, J. Y. Wang, M. H. Jiang, R. I. Boughton, D. G. Ran, S. Q. Sun, and H. R. Xia

Citation: Journal of Applied Physics **100**, 063513 (2006); doi: 10.1063/1.2335510
View online: http://dx.doi.org/10.1063/1.2335510
View Table of Contents: http://scitation.aip.org/content/aip/journal/jap/100/6?ver=pdfcov
Published by the AIP Publishing

Growth and thermal properties of $SrWO_4$ single crystal

J. D. Fan, H. J. Zhang,[a] J. Y. Wang, and M. H. Jiang
State Key Laboratory of Crystal Materials, Shandong University, Jinan 250100, People's Republic of China and Institute of Crystal Materials, Shandong University, Jinan 250100, People's Republic of China

R. I. Boughton
Department of Physics and Astronomy, Bowling Green State University, Ohio 43403

D. G. Ran, S. Q. Sun, and H. R. Xia
Department of Physics, Shandong University, Jinan 250100, People's Republic of China

(Received 25 October 2005; accepted 6 June 2006; published online 22 September 2006)

A strontium tungstate ($SrWO_4$) single crystal with dimensions of $\Phi\ 25\times40\ mm^2$ has been grown by the Czochralski method using an iridium crucible. X-ray powder diffraction results show that as grown the $SrWO_4$ crystal belongs to the tetragonal system in the scheelite structure. The effective segregation coefficients of elemental W and Sr in the crystal growth are measured by x-ray fluorescence, and the respective values are close to 1. The thermal properties of the $SrWO_4$ crystal were systemically studied by measuring the thermal expansion, specific heat, and thermal diffusion coefficient. These results show that the crystal possesses a large anisotropic thermal expansion with thermal-expansion coefficients $\alpha_a=8.61\times10^{-6}/K$, $\alpha_b=8.74\times10^{-6}/K$, $\alpha_c=18.78\times10^{-6}/K$ over the temperature range of 303.15–773.15 K. The measured value of the specific heat is 0.30–0.34 $J\ g^{-1}\ K^{-1}$ when the temperature is increased from 323.15 to 1073.15 K. The thermal diffusion coefficient was measured over the temperature range of 303.15–543.15 K. The thermal conductivities of the $SrWO_4$ crystal along the [100] and [001] directions are calculated to be 3.1326 $W\ m^{-1}\ K^{-1}$ and 2.9477 $W\ m^{-1}\ K^{-1}$, respectively, at 303.15 K. Then the thermal properties of some other Raman crystals were compared with these data, and the thermal focal lengths for these crystals were also estimated. © *2006 American Institute of Physics*. [DOI: 10.1063/1.2335510]

I. INTRODUCTION

The search for efficient crystal materials for stimulated Raman scattering (SRS) and the study of SRS lasers are significant because of the need for laser radiation sources that operate efficiently in new spectral regions. All-solid-state Raman lasers based on SRS can radiate over a wide emission range from ultraviolet to near infrared, depending on the pump laser wavelength and on the type of Raman-active crystal being used. Raman-active crystals, such as $Ba(NO_3)_2$, $KGd(WO_4)_2$ (KGW), $BaWO_4$, and $SrWO_4$, have attracted a great deal of attention in recent years because of their excellent properties.[1–10] The study of the alkaline-earth tungstate crystals by means of spontaneous Raman spectroscopy and SRS has made it possible to predict and confirm that $SrWO_4$ is a good prospect for an all-solid-state Raman laser.[7,11–14]

The growth of pure and rare-earth-doped $SrWO_4$ crystals has been reported in the literature.[7,11–14] In addition, the regression data and percentage expansion data for the $SrWO_4$ crystal were given by Taylor in 1986[15] and the thermal expansion data for the $Tm^{3+}:SrWO_4$ crystal were measured in the literature.[16] The mean thermal capacity of the $SrWO_4$ crystal was measured by Zharkova and Rezukhina with a massive calorimeter in 1958.[17] However, the thermal properties of the pure $SrWO_4$ crystal including thermal expansion, specific heat, and especially the thermal conductivity have not been systemically studied, and this may limit the study of $SrWO_4$ for Raman laser applications. For a specific crystal the thermal properties are the most important in modeling crystal growth and laser design. If a crystal possesses a large anisotropic thermal expansion, it may easily crack during crystal growth and crystal processing when the temperature gradient is excessive. During the operation of a Raman laser, the Raman-active crystal absorbs energy from the pump source, and this energy is deposited as heat due to the inelastic nature of the SRS process (thermal loading). Thermal loading must be taken into account in the design of Raman lasers, especially for scaling the devices up to higher average power.[5] Thermal loading causes a temperature gradient in the crystal and leads to thermal expansion, which in turn produces thermal lensing and other thermo-optic effects. All the effects related to thermal loading reduce the quality of the laser beam and may even lead to cracking of the Raman-active crystal. The specific heat is an important factor that affects the damage threshold of the material.[18] Another important quantity to calculate is the thermal conductivity. If the Raman-active crystal possesses a high thermal conductivity, the deposited heat can easily be transferred to the environment, thus decreasing the thermal loading effects and opening up the possibility of pumping the crystal at high repetition rates (~10 kHz).[19] However, no reports on the thermal conductivity of crystalline $SrWO_4$ have been found in a search of the literature. Consequently, a study of the thermal properties of crystalline $SrWO_4$ will most likely provide useful information for Raman laser designs.

The aim of this paper is to report the results of $SrWO_4$

[a]Author to whom correspondence should be addressed; electronic mail: hjzhang@icm.sdu.edu.cn

single crystal growth as well as its thermal properties, including thermal expansion, specific heat, and thermal conductivity. With this data in hand, the thermal properties of some other Raman crystals were compared, and their thermal focal lengths were estimated.

II. EXPERIMENT

The polycrystalline precursor materials used for growing single crystal $SrWO_4$ were prepared by a solid-phase reaction. $SrCO_3$ and WO_3 compounds with 99.99% purity were combined according to the stoichiometric ratio of $SrWO_4$, and an additional 1–2 wt % WO_3 was added to compensate for the volatilization of WO_3 in the processes of synthesizing the polycrystalline materials and single crystal growth. After the compounds were ground and mixed, they were put into a platinum crucible and were heated to 1273 K for 10 h to decompose the carbonate and form polycrystalline $SrWO_4$. The polycrystalline material was ground and mixed again, and then pressed into a cylindrical shape with dimensions of $\Phi\ 50\times40\ mm^2$. It was then sintered using the same procedure as in the first step above.

A. Crystal growth

A $SrWO_4$ single crystal was grown in an iridium (Ir) crucible, which is 66 mm in diameter and 40 mm in height, and which contained about 350 g of polycrystalline $SrWO_4$. The Ir crucible was heated by using a 2 kHz intermediate frequency furnace. The temperature-control apparatus was Eurotherm 818 controller/programmer with a precision of ±0.5 K. The crawling distance of the pulling apparatus was less than 1 μm, and the growth atmosphere was N_2. Initially, a randomly oriented crystal was obtained from a polycrystalline nucleation at the end of a platinum-rhodium (Pt–Rh) rod by restricting the diameter of the material so that only one crystal could be grown. Then an *a*-axis rectangular $SrWO_4$ single crystal bar with dimensions of $3\times3\times20\ mm^3$, cut from the as-grown crystal boule, was used as a seed for subsequent growth. In order to avoid the formation of polycrystals during the growth process, a temperature of 30–50 K higher than the melting point of polycrystalline $SrWO_4$ (the melting point of $SrWO_4$ is 1808 K[12]) was initially maintained for 1 hour to melt the microcrystalline particles in the Ir crucible. The temperature was then lowered to the melting temperature. The seed was necked down before it was tapered off to a diameter of about 1 mm. The pulling rate was 0.5–1.5 mm/h and the rotation rate was fixed at 12 rpm during the entire crystal growth process. After the growth was completed, the crystal was cooled down to room temperature at a rate of 30 K/h.

In order to eliminate the remnant thermal stress and the color centers produced in the growth process due to oxygen deficiency, the as-grown $SrWO_4$ crystal boule was annealed according to the following procedure: The crystal was first put into a constant temperature field in an annealing furnace and slowly heated to 1273 K in air. It was maintained at that temperature for 10 h, and then was cooled down to room temperature at a low rate of about 30 K/h.

B. X-ray powder diffraction

The x-ray powder diffraction (XRPD) method was used to determine the lattice structure and lattice parameters of the $SrWO_4$ crystal. A small portion of the crystal was ground into a fine powder and used as a sample in the XRD apparatus (Rigaku D/MAX 2200PC) using the Cu Kα lines ($\alpha = 1.5418\times10^{-10}$ m).

C. Effective segregation coefficient measurements

The x-ray fluorescence analysis method was used to measure the concentrations of elemental Sr and W in the $SrWO_4$ single crystal. Based on the measurements, the effective segregation coefficients of elemental Sr and W in the crystal growth process were calculated. The measured samples were cut from the upper and lower portions of the $SrWO_4$ crystal and were ground into powder. The polycrystalline material used for growing the $SrWO_4$ crystal was employed as a comparison sample.

D. Thermal-expansion measurements

The thermal expansion of the $SrWO_4$ crystal was measured over the temperature range of to 303.15–773.15 K by using a thermal dilatometer (Perkin Elmer). The crystal used for the thermal-expansion measurement was processed into a rectangular sample with dimensions of $7.06\times6.31\times6.32\ mm^3$ ($a\times b\times c$). During the thermal-expansion measurements, the sample was heated at a constant rate of 5 K/min from 303.15–773.15 K, and thermal-expansion ratio versus temperature curves along the *a*-, *b*- and *c*-crystallographic axes were measured.

E. Specific-heat measurements

The specific heat was measured by the method of differential scanning calorimetry using a simultaneous thermal analyzer (NETZSCH DSC 404C) through the following steps: An empty sample Pt–Rh crucible together with another empty reference Pt–Rh crucible were heated from 323.15 to 1073.15 K at a constant rate of 10 K/min in order to determine the base line. Then a sapphire calibration sample weighing 41 mg was placed in the sample Pt–Rh crucible and was heated together with the other empty reference Pt-Rh crucible. Finally, a $SrWO_4$ sample weighing 68.25 mg was placed in the sample crucible and was heated together with the other empty reference Pt–Rh crucible through the same range as above. As a result, the specific heat of the $SrWO_4$ crystal could be calculated using a comparison method with the CP software package provided by the NETZSCH Company.

F. Thermal diffusion coefficient measurements

The thermal diffusion coefficients of the $SrWO_4$ crystal were measured by the laser flash method using a laser flash apparatus (NETZSCH LFA 447 Nanoflash) over the temperature range of 303.15–543.15 K. Two square wafers ($6.000\times6.000\times2.880$ and $6.000\times6.000\times2.670\ mm^3$) having polished faces perpendicular to the [100] and [001] crystallographic axes, and coated with graphite on both sides,

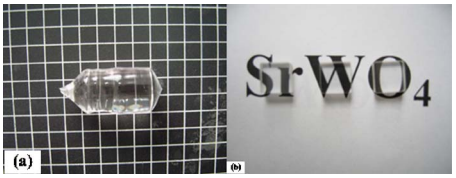

FIG. 1. The as-grown $SrWO_4$ crystal boule and polished sections.

were used to carry out the measurements. During the experiment, a short pulse of light heats the front surface of the plane-parallel $SrWO_4$ wafer, and the temperature rise on the rear surface is measured as a function of time using an IR detector. The thermal diffusion coefficient of the crystal was calculated using analytical software provided by the NETZSCH Company.

III. RESULT AND DISCUSSION

A. Crystal growth and structure characterization

Figures 1(a) and 1(b) show the as-grown $SrWO_4$ crystal boule using an *a*-axis seed and the polished sections of the crystal, respectively. The dimensions of the $SrWO_4$ crystal boule are about Φ 25×40 mm^2. There are no low angle boundaries, no inclusions, and no other macroscopic defects in the crystal. Moreover, no light-scattering centers were observed when the crystal was illuminated using a 10 mW He–Ne laser. All of these results mean that the $SrWO_4$ crystal possesses good optical quality and is therefore suitable for Raman laser applications.

Figures 2(a) and 2(b) show the XRPD patterns of the $SrWO_4$ crystal and the standard XRPD reference card for $SrWO_4$,[20] respectively. It can be seen that the XRPD pattern of the crystal is in good agreement with the standard reference. This comparison suggests that the $SrWO_4$ crystal possesses the scheelite structure and belongs to the tetragonal system and $I4_1/a$ space group. The unit-cell parameters were calculated from the XRPD data, and they are $a=b=5.4078\times10^{-10}$ m and $c=11.9316\times10^{-10}$ m. These results are similar to the standard parameters of $SrWO_4$, which are $a=b=5.4168\times10^{-10}$ m and $c=11.951\times10^{-10}$ m.[20]

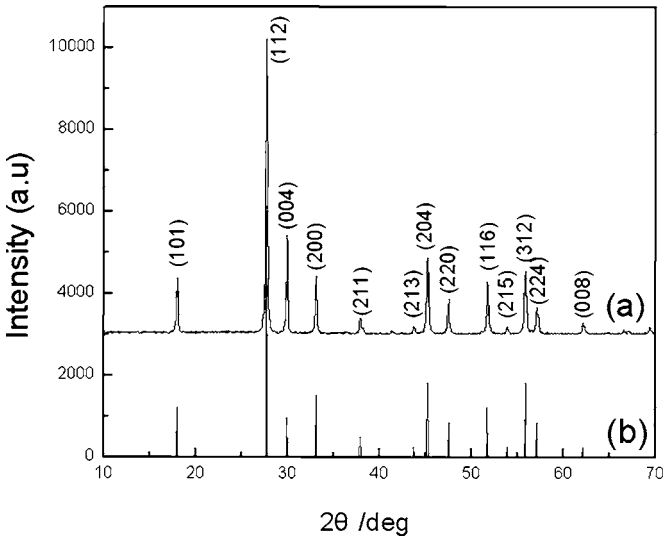

FIG. 2. X-ray powder diffraction patterns: (a) as-grown $SrWO_4$ crystal; (b) JCPDS Diffraction File Card No. 08-0490 (Ref. 20).

TABLE I. The effective segregation coefficient (K_{eff}) of elements in $SrWO_4$.

	Upper	Lower
K_{eff}(Sr)	0.9887	1.0283
K_{eff}(W)	0.9654	1.0150

Table I shows the effective segregation coefficients of elemental Sr and W in $SrWO_4$ crystal growth. From Table I, it can be seen that the segregation coefficients of Sr and W are very close to unity. Since the density of W ion is larger than that of Sr ion, the effective segregation coefficient of Sr is larger than that of W in the upper and lower parts of the as-grown $SrWO_4$ crystal. The volatilization of WO_3 during the process of crystal growth could also account for the fact that the effective segregation coefficient of Sr is larger than that of W. Therefore, the compensation of 1–2 wt % WO_3 is important in order to obtain a uniform $SrWO_4$ single crystal.

B. Thermal expansion

The thermal-expansion coefficient (α_{ij}) of a crystal is a symmetric second-rank tensor,[21] and it can be described by the representation quadric. Measurements of thermal expansion have greatly increased our knowledge of material properties such as lattice dynamics, electronic and magnetic interactions, thermal defects, and phase transitions.[22]

$SrWO_4$ crystal belongs to the tetragonal system and $4/m$ point group. The unique symmetry axis is a fourfold axis along the crystallographic *c* axis; the axes of the crystallographic and crystallophysical coordinate systems in $SrWO_4$ have the same direction, that is, $a\|X_1$, $b\|X_2$, and $c\|X_3$. It is well known that there are only two independent principal components of the thermal-expansion coefficient tensor in a tetragonal system and the components are $\alpha_1=\alpha_2$ (along *a* or *b* axis) and α_3 (along *c* axis).

The solid lines in Fig. 3 are the thermal-expansion ratio curves along the crystallographic axes. It can be seen that the

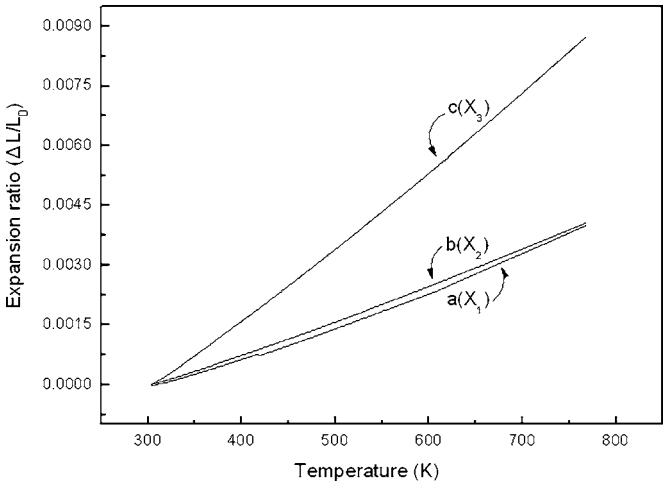

FIG. 3. Thermal-expansion ratio curves of $SrWO_4$ crystal.

expansion ratio is almost linear over the entire measured temperature range and the $SrWO_4$ crystal exhibits expansion when it is heated.

The average linear thermal-expansion coefficient for the crystallographic directions can be calculated according to the following formula:

$$\bar{\alpha}(T_0 \rightarrow T) = \frac{\Delta L}{L_0}\frac{1}{\Delta T}, \tag{1}$$

where $\bar{\alpha}(T_0 \rightarrow T)$ is the average linear thermal-expansion coefficient over the temperature range of T_0 to T, L_0 is the sample length at T_0, ΔL is the length change when the temperature changes from T_0 to T, and the temperature change is $\Delta T = T - T_0$.

The values of the average linear thermal-expansion coefficients of the $SrWO_4$ crystal over the temperature range of 303.15–773.15 K are $\alpha_a = 8.61 \times 10^{-6}/\mathrm{K}$, $\alpha_b = 8.74 \times 10^{-6}/\mathrm{K}$, $\alpha_c = 18.78 \times 10^{-6}/\mathrm{K}$. The expansion coefficient in the [001] direction is about 2.2 times larger than that in the [100] or [010] directions according to our experimental results, which means that crystalline $SrWO_4$ has a large and anisotropic thermal expansion. The value of α_c/α_a in our experiment is similar to the value (2.4) in Ref. 16. Nevertheless, the absolute values for α_a, α_b, and α_c are significantly different (their results are $\alpha_a = 1.01 \times 10^{-5}/\mathrm{K}$, $\alpha_b = 1.01 \times 10^{-5}/\mathrm{K}$, $\alpha_c = 2.4 \times 10^{-5}/\mathrm{K}$). The reasons for the difference could be discussed as follows: (1) In Ref. 16, the measured crystal was $Tm^{3+}:SrWO_4$, which is different from our pure $SrWO_4$ crystal. (2) The reported thermal-expansion coefficients in Ref. 16 were measured in the temperature range of 300–1300 °C, which is different from our range of 25–500 °C. In addition, the working temperature range of all-solid-state Raman lasers is from 25 to 300 °C, suggesting that thermal expansion measurements in this temperature range have more applications. (3) The measured crystal was heated at a rate of 5 °C/min in our experiment, which is different from their 10 °C/min. (4) The difference of the measure apparatus and the measured crystal might cause the experimental errors.

C. Specific heat

Figure 4 shows the specific heat versus temperature curve of the $SrWO_4$ crystal. It can be seen that the specific heat of the crystal is almost linear and has little variation over the temperature range of 323.15–1073.15 K. This means that temperature change has little influence on the specific heat of the crystal over the temperature range of the measurements.

The specific-heat value of the crystal ranges from 0.30–0.34 $\mathrm{J\,g^{-1}\,K^{-1}}$ when the temperature is increased from 323.15 to 1073.15 K, and is the equivalent of 100.64–114.06 $\mathrm{J\,K^{-1}\,mol^{-1}}$. According to Kopp's law, the specific heat of 1 mol of a substance is a sum over all atomic vibrational modes, and is calculated to be 116.8 $\mathrm{J\,K^{-1}\,mol^{-1}}$.[23] The measured value is almost in agreement with the calculated value. It is similar to crystalline $BaWO_4$.[23] The specific heat of crystalline $SrWO_4$ is in compliance with the Dulong-Petit law, and the Debye temperature of the crystal is apparently no higher than 323.15 K.[24]

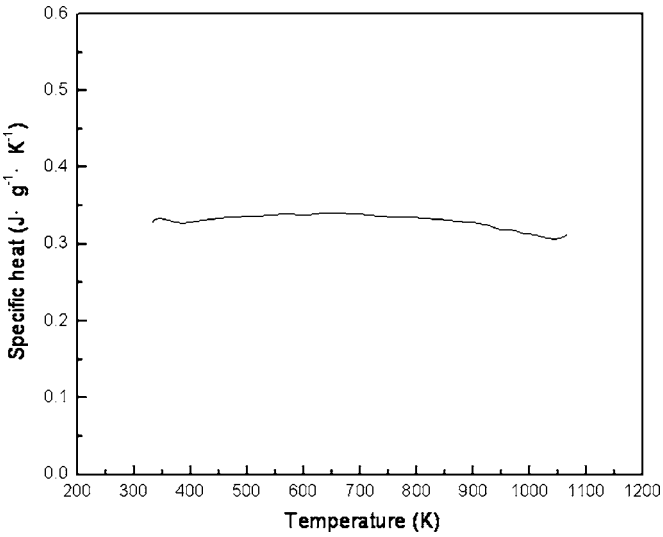

FIG. 4. Specific heat vs temperature curve of $SrWO_4$ crystal.

D. Thermal diffusion coefficient and thermal conductivity

The thermal conductivity (κ_{ij}) of a crystal is also a symmetric second-rank tensor.[21] Just as in the case of the thermal-expansion coefficient tensor, the (κ_{ij}) tensor also has only two independent principal components for a tetragonal system, which can be obtained by making measurements on *a*- and *c*-oriented samples.

The thermal conductivity κ of crystalline $SrWO_4$ was calculated using the measured thermal diffusion coefficient and specific heat according to the following equation:

$$\kappa = \lambda \rho C_p, \tag{2}$$

where λ, C_p, and ρ denote the thermal diffusion coefficient, specific heat, and density of the crystal, respectively.

The solid lines in Fig. 5 show the thermal diffusion co-

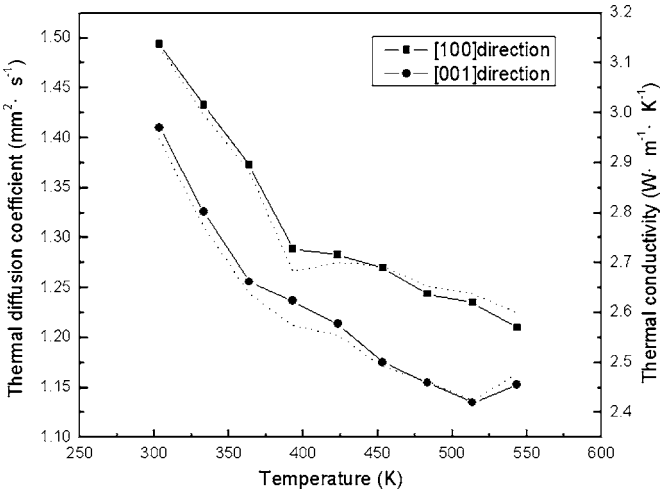

FIG. 5. Solid lines: Thermal diffusion coefficient of $SrWO_4$ crystal. Dotted lines: The calculated thermal conductivity of $SrWO_4$ crystal.

TABLE II. Some thermal property parameters of several Raman crystals. [Note: Crystal growth method, aqueous (aqueous method), flux (flux method), and Cz (Czochralski method).]

Crystal	$Ba(NO_3)_2$	KGW	KLuW	$BaWO_4$	SrO_4	YVO_4	$GdVO_4$
Thermal	1.17	2.6[100]	3.09	2.256	3.133	5.1	11.4
coductivity		3.8[010]	2.55	2.324	2.948	5.23	10.7
(W/m K)		3.4[001]	4.4				
Thermal-expansion	13	4[100]	12.8	10.9	8.61	2.2	1.5
coefficient (10^{-6} K)		1.6[010]	7.8	35.1	18.78	8.4	7.3
		8.5[001]	22.2				
Specific heat (J/K mol)	···	346.02	259.07	115.56	100.64	22.6	32.6
Thermal optical	−20	−0.8	···	···	···	3	4.7
coefficient dn/dT (10^{-6})		−5.5					
Refractive index	1.55	2	2	1.8	1.8	2	2
Crystal growth method	Aqueous	Flux	Flux	Cz	Cz	Cz	Cz

efficients of the crystal over the temperature range of 303.15–543.15 K at 30 K interval between measured temperature points. The dotted lines in Fig. 5 show the thermal-conductivity components of the $SrWO_4$ crystal at corresponding temperatures.

It is clearly shown in Fig. 5 that the thermal diffusion components and thermal-conductivity components of the $SrWO_4$ crystal decrease with increasing temperature. The thermal diffusion coefficients of the crystal are 1.494 $mm^2\,s^{-1}$ along the [100] direction and 1.41 $mm^2\,s^{-1}$ along the [001] direction at 303.15 K. Correspondingly, the calculated thermal-conductivity components of the crystal are 3.1326 $W\,m^{-1}\,K^{-1}$ along the [100] direction and 2.9477 $W\,m^{-1}\,K^{-1}$ along the [001] direction at 303.15 K. These results show that $SrWO_4$ has a higher thermal conductivity than $BaWO_4$ (Ref. 23) and $Ba(No)_3$ (Ref. 5) at the same temperature, and so crystalline $SrWO_4$ is suitable for high power Raman laser applications.

E. Comparison of thermal properties and thermal focal lengths of $SrWO_4$ with other Raman crystals

Thermal problems are important in laser system. Optical pumping of all-solid-state lasers generates some amount of localized heating in the laser material. Under operating conditions the thermally loaded laser host medium can exhibit optical distortions, which include thermal focusing, stress-induced biaxial focusing and stress-induced birefringence. The thermally induced effects severely degrade the optical quality of the laser beam and eventually limit the laser output power. The combined effects of volumetric heating and surface cooling can result in thermal-mechanical failure from stress.

The fraction of the pump power that is converted to heat strongly depends on the choice of laser material and of the corresponding pump source.[25,26] The thermal effects can be presented by the thermal lensing effect, and the thermal focal length f can be written as[27]

$$f = \frac{\kappa A}{P_a}\left[\frac{1}{2}\frac{dn}{dT} + \alpha C_{r,\phi} n_0^3 + \frac{\alpha r_0 (n_0 - 1)}{L}\right]^{-1}, \tag{3}$$

where κ is the thermal conductivity, A is the rod cross-sectional area, P_a is the total heat dissipated in the rod, dn/dt is the temperature coefficient of index of refraction, n_0 is the index of refraction, $C_{r,\phi}$ is the photoelastic coefficient, α is the thermal-expansion coefficient, r_0 is the radius of the crystal, and L is the length of the rod.

Table II shows thermal properties of seven important Raman crystals: $Ba(NO_3)_2$ KGW, $KLu(WO_4)_2$ (KLuW), $BaWO_4$, $SrWO_4$, YVO_4, and $GdVO_4$.[5,28–35] From Table II, we can see that $SrWO_4$ has a larger thermal conductivity than $BaWO_4$, and the anisotropy in the thermal-expansion coefficients of $SrWO_4$ is smaller than in $BaWO_4$. The larger thermal conductivity and lower anisotropy in the thermal expansion of $SrWO_4$ make it more preferable for use in higher power laser systems than $BaWO_4$. Crystalline $SrWO_4$ will exhibit a more stable laser output when it is used as a Raman crystal.

By using Table II and formula (3), we can estimate the thermal focal lengths of the seven different Raman crystals. In formula (3), the dn/dT value is most important in all of the parameters to calculate the thermal focal lengths. For $BaWO_4$ and $SrWO_4$, we used the dn/dT value of $CaWO_4$;[5] for KLuW crystal, we used the dn/dT value of KGW. We suppose that all the crystals have the same cross-sectional area (A). For Raman laser, the heat comes from the transformation of a pumping laser to a Raman laser, and the Raman shift wavelengths are almost the same for the seven different Raman crystals. Therefore, we can also suppose that they have the same total heat dissipated in the rod (P_a). The pho-

TABLE III. Relative thermal focal lengths of seven Raman crystals. (Note: for $r_0/L=1/5$, take $1.095\times10^5 A/P_a$ as 1; for $r_0/L=1/10$, take $1.073\times10^5 A/P_a$ as 1.

Crystal	$Ba(NO_3)_2$	KGW	KLuW	$BaWO_4$	$SrWO_4$	YVO_4	$GdVO_4$
($r_0/L=1/5$)	1	16.16	13.88	5.21	6.32	35.53	45.66
($r_0/L=1/10$)	1	13.88	8.59	3.63	5.34	60.21	58.15

toelastic coefficients ($C_{r,\phi}$) have less influence on the thermal focal lengths, and what is more, the photoelastic coefficients of these crystals are four-rank tensor and they are not easy to be obtained, so we have used the photoelastic coefficient $C_{r,\phi}=0.029$ of crystalline yttrium aluminum garnet (YAG) in all seven cases.[36] The thermal-expansion coefficient, thermal conductivity, and thermal optical coefficient used are the average values for each crystal. For example, the thermal conductivity of KGW is $(2.6+3.8+3.4)/3=3.27$. Table III shows the calculated $|f|$ values of the seven Raman crystals when $r_0/L=1/5$ and $1/10$. From Table III we can see that $Ba(NO_3)_2$ has the strongest thermal lensing effect of all seven crystals, and the vanadate crystals are the best. KGW and KLuW are also very good Raman crystals, but these crystals are grown by the flux method, and this may limit the crystal dimensions since the crystal growth can take a long time.[37,38] Vanadate crystals show a weak thermal lensing effect when they are used as Raman crystals, so vanadate crystals may be very excellent for this purpose, but they have a high melting point and crystal growth of large dimension boules is very difficult.[39–41] This property may also limit the applications of vanadate crystals where large crystal dimensions are required. $BaWO_4$ and $SrWO_4$ crystals have a strong thermal lensing effect, but these crystals have a low melting point and are easily grown, so large dimension crystals (longer than 80 mm) can be obtained by using the Czochralski method.[23] $BaWO_4$ and $SrWO_4$ crystals have high Raman gain, and all these properties make $BaWO_4$ and $SrWO_4$ widely used as Raman crystals. $SrWO_4$ has a higher thermal conductivity than $BaWO_4$, and this means that $SrWO_4$ has more potential applications in high power systems.

IV. CONCLUSIONS

A transparent $SrWO_4$ single crystal with good quality was grown by the Czochralski method. The thermal properties of $SrWO_4$ were carefully studied by measuring thermal expansion, specific heat, and thermal conductivity. The average linear thermal-expansion coefficients calculated according to the thermal-expansion measurements are $\alpha_a=8.61\times10^{-6}/\mathrm{K}$, $\alpha_b=8.74\times10^{-6}/\mathrm{K}$, and $\alpha_c=18.78\times10^{-6}/\mathrm{K}$. The specific heat of the crystal is little changed at a measured value of 0.30–0.34 J g^{-1} K^{-1} over the temperature range of 323.15–1073.15 K. The calculated thermal-conductivity components of the crystal are 3.1326 W m^{-1} K^{-1} along the [100] direction and 2.9477 W m^{-1} K^{-1} along the [001] direction at 303.15 K. Then the thermal properties of $SrWO_4$ were compared with other Raman crystals, and the thermal focal lengths of these crystals were also estimated.

ACKNOWLEDGMENTS

This work is supported by the Grant for State Key Program of China (2004CB619002) and the National Natural Science Foundation of China (Grant No. 50590401)

[1] P. G. Zverev, T. T. Basiev, V. V. Osiko, A. M. Kulkov, V. N. Voitsekhovskii, and V. E. Yakobson, Opt. Mater. (Amsterdam, Neth.) **11**, 315 (1999).
[2] P. G. Zverev, T. T. Basiev, and A. M. Prokhorov, Opt. Mater. (Amsterdam, Neth.) **11**, 335 (1999).
[3] J. Findeisen, H. J. Eichler, and P. Peuser, Opt. Commun. **181**, 129 (2000).
[4] P. Cerny, P. G. Zverev, H. Jelınkova, and T. T. Basiev, Opt. Commun. **177**, 397 (2000).
[5] H. M. Pask, Prog. Quantum Electron. **27**, 3 (2003).
[6] T. T. Basiev, A. A. Sobol, Yu. K. Voronko, and P. G. Zverev, Opt. Mater. (Amsterdam, Neth.) **15**, 205 (2000).
[7] G. Jia, C. Tu, Z. You, J. Li, Z. Zhu, Y. Wang, and B. Wu, J. Cryst. Growth **273**, 220 (2004).
[8] P. Cerny, H. Jelinkova, P. G. Zverev, and T. T. Basiev, Prog. Quantum Electron. **28**, 113 (2004).
[9] T. T. Basiev, A. A. Sobol, P. G. Zverev, V. V. Osiko, and R. C. Powell, Appl. Opt. **38**, 594 (1999).
[10] W. Ge, H. Zhang, J. Wang, J. Liu, X. Xu, X. Hu, J. Li, and M. Jiang, J. Cryst. Growth **270**, 582 (2004).
[11] P. G. Zverev, T. T. Basiev, A. A. Sobol, V. V. Skornyakov, L. I. Ivleva, N. M. Polozkov, and V. V. Osiko, Quantum Electron. **30**, 55 (2000).
[12] L. I. Ivleva, T. T. Basiev, I. S. Voronina, P. G. Zverev, V. V. Osiko, and N. M. Polozkov, Opt. Mater. (Amsterdam, Neth.) **23**, 439 (2003).
[13] A. Brenier, G. Jia, and C. Tu, J. Phys.: Condens. Matter **16**, 9103 (2004).
[14] H. Jelinkova, J. Sulc, T. T. Basiev, P. G. Zverev, and S. V. Kravsov, Laser Phys. Lett. **2**, 4 (2005).
[15] D. Taylor, Br. Ceram. Trans. J. **85**, 147 (1986).
[16] G. Jia, C. Tu, Z. You, J. Li, Z. Zhu, and B. Wu, Solid State Commun. **134**, 583 (2005).
[17] L. A. Zharkova and T. N. Rezukhina, Zh. Fiz. Khim. **32**, 2233 (1958).
[18] D. Xu, in *Science and Technology of Crystal Growth*, edited by K. C. Zhang and L. H. Zhang (Science, Beijing, 1997), in Chinese.
[19] P. Cerny, H. Jelinkova, M. Miyagi, T. T. Basiev, and P. G. Zverev, Proc. SPIE **4630**, 108 (2002).
[20] JCPDS Diffraction File Card No. 08-0490, 1999 (unpublished).
[21] J. F. Nye, *Physical Properties of Crystals* (Oxford University Press, Oxford, 1985).
[22] H. Choosuwan, R. Guo, A. S. Bhalla, and U. Balachandran, J. Appl. Phys. **91**, 5051 (2002).
[23] W. W. Ge, H. J. Zhang, J. Y. Wang, J. H. Liu, X. G. Xu, X. B. Hu, and M. H. Jiang, J. Appl. Phys. **98**, 013542 (2005).
[24] M. Born and K. Huang, *Dynamical Theory of Crystal Lattices* (Oxford University Press, Oxford, 1954).
[25] T. Y. Fan, IEEE J. Quantum Electron. **26**, 1457 (1993).
[26] R. Weber, B. Neuenschwander, M. Mac Donald, M. B. Toos, and H. P. Weber, IEEE J. Quantum Electron. **34**, 1046 (1998).
[27] W. Koechner, *Solid-State Laser Engineering* (Springer-Verlag, Berlin, 1996).
[28] P. G. Zverev, T. T. Basiev, V. V. Osiko, A. M. Kukov, V. N. Voitekhovskii, and V. E. Yakobson, Opt. Mater. (Amsterdam, Neth.) **11**, 315 (1999).
[29] I. V. Mochalov, Opt. Eng. (Bellingham) **36**, 1660 (1997).
[30] J. Zhang *et al.*, Appl. Phys. Lett. **87**, 061104 (2005).
[31] H. Zhang, L. Zhu, X. Meng, Z. Yang, C. Wang, W. Yu, Y. Chow, and M. Lu, Cryst. Res. Technol. **34**, 1011 (1999).
[32] H. Zhang, J. Liu, J. Wang, C. Wang, L. Zhu, Z. Shao, X. Meng, X. Hu, M. Jiang, and Y. Chow, J. Opt. Soc. Am. B **19**, 18 (2002).
[33] A. Kaminskii *et al.*, Opt. Commun. **194**, 201 (2001).
[34] B. Chai, G. Loutts, J. Lefaucheur, X. Zhang, P. Hong, M. Bass, I. Shcherbakov, and A. Zagumennyi, OSA Trends Opt. Photonics Ser. **20**, 41 (1994).
[35] L. Qin, X. Meng, H. Shen, L. Zhu, B. Xu, H. Xia, P. Zhao, and G. Zheng, Cryst. Res. Technol. **38**, 793 (2003).
[36] R. W. Dixon, J. Appl. Phys. **38**, 5149 (1967).
[37] G. Wang and Z. Luo, J. Cryst. Growth **102**, 765 (1990).
[38] R. Sole, V. Nikolov, X. Ruiz, J. Cavalda, X. Solans, M. Agvobo, and F. Diaz, J. Cryst. Growth **169**, 600 (1996).
[39] S. Erdei, J. Cryst. Growth **134**, 1 (1993).
[40] X. Meng, L. Zhu, H. Zhang, C. Wang, Y. Chow, and M. Lu, J. Cryst. Growth **200**, 199 (1999).
[41] S. Wu, G. Wang, and J. Xie, J. Cryst. Growth **266**, 496 (2004).